

Chapter 6

Heat budgets of the Leeuwin Current System

6.1 INTRODUCTION

The aim of this chapter is to quantify the ocean heat balance of the Leeuwin Current and southeast Indian Ocean off Western Australia (22°S–34°S, east of 107°E) using the POP11B model outputs 1993/97 [**Appendix C**], and to identify the dominant mechanism leading to the cooling of the Leeuwin Current [$\sim 0.6^\circ\text{C}$ per 100 km, as found in **Chapter 5**].

6.2 BOX METHOD

Conservation of heat implies that the divergence of the ocean heat in a closed box, with no net mass flux, must equal the net heat exchange with the atmosphere over the surface area of the box (diffusion is generally small and storage is zero in a steady state ocean) [e.g., Montgomery, 1974; Wyrтки, 1981; Bryden and Brady, 1985; Enfield, 1986]. So, following this approach, heat budgets were carried out for the two boxes defined in **Figure 6.1**, from the surface to the bottom of the ocean. The coastal box covers the main jet of the Leeuwin Current and shelf waters whereas the offshore box includes the ocean interior adjacent to the Leeuwin Current and that part of the southeast Indian Subtropical Gyre east of 107°E. To provide a regional perspective of the heat balance, off Western Australia, we have also calculated budgets for a series of $1^\circ \times 1^\circ$ boxes over the area in question.

The total ocean heat divergences were divided by the surface area of the boxes and reported in units of W m^{-2} so that they are directly comparable with spatial averages of the ocean–atmosphere flux at the box surface [**Table 6.1**]. The residual between the ocean–atmosphere exchange and the heat divergence by the currents was taken as the “storage + diffusion” term as we cannot explicitly determine diffusion effects from the

available model outputs. As expected this “storage + diffusion” term is a very small part of the 5–year averaged heat balance. Although the net surface flux and the total ocean heat transport are directly available from the model, we have carried out a Reynolds decomposition of the ocean heat transport to elucidate mechanisms.

The total ocean heat transport was separated into that carried by the 5–year mean, seasonal, interannual and “eddy” components of velocity and θ fields [Equation 6.1]. The transients account for the correlations between the temporal fluctuations of the velocity and θ fields on different timescales. The “eddy” term refers to any heat flux anomaly that is not included in the seasonal and interannual frequencies, therefore it essentially comprises the fluxes due to correlations on submonthly timescales. By carrying out this partition of the total ocean heat transport (which has more terms than usual) our aim was to find out whether seasonal rectification was an important part of the budget, considering the evident seasonal cycle of the Leeuwin Current along the west Australian coast [the warmest tropical waters and the strongest poleward transport are both observed during May–June, see Chapter 5].

The terms of the ocean heat transport in Equation 6.1 were determined from the model outputs for each grid point except the eddy term ($\mathbf{U}'\Theta'$), which was indirectly inferred as the residual of all of the other terms. These terms were then integrated from top to bottom across the box boundaries to provide an estimate of the ocean heat divergence [Table 6.1]. Prior to these calculations we have certified that there was no net volume (mass) flux in the coastal and offshore boxes [Table 6.1] and likewise for the $1^\circ \times 1^\circ$ boxes [Appendix D].

$$\langle \mathbf{U}\Theta \rangle = \langle \mathbf{U} \rangle \langle \Theta \rangle + \langle \mathbf{U}_s' \Theta_s' \rangle + \langle \mathbf{U}_i' \Theta_i' \rangle + \langle \mathbf{U}_s' \Theta_i' \rangle + \langle \mathbf{U}_i' \Theta_s' \rangle + \langle \mathbf{U}' \Theta' \rangle \quad [\text{Equation 6.1}]$$

where:

\mathbf{U} is the cross–sectional velocity component

Θ is heat (ρC_p)

$\rho = 1025 \text{ kg m}^{-3}$ (mean density)

$C_p = 3989 \text{ J kg}^{-1} \text{ }^\circ\text{C}^{-1}$ (heat capacity)

$\langle \rangle$ 5–year average

$_s'$ seasonal fluctuations

$_i'$ interannual fluctuations

$'$ submonthly fluctuations

6.3 HEAT BUDGETS

The southeast Indian Ocean off Western Australia (22°–34°S and 100°–115°E) releases a considerable amount of heat to the overlying atmosphere as implied by the 5-year mean surface heat flux field in **Figure 6.1**. The ocean heat loss is largest within the coastal box, associated with the boundary poleward path of the Leeuwin Current (–50 to –70 W m^{-2}). Away from the coastal boundary, the ocean heat loss gradually tapers to about –20 W m^{-2} along the western rim of the offshore box. How this implied heat is balanced by the heat ocean components is detailed below.

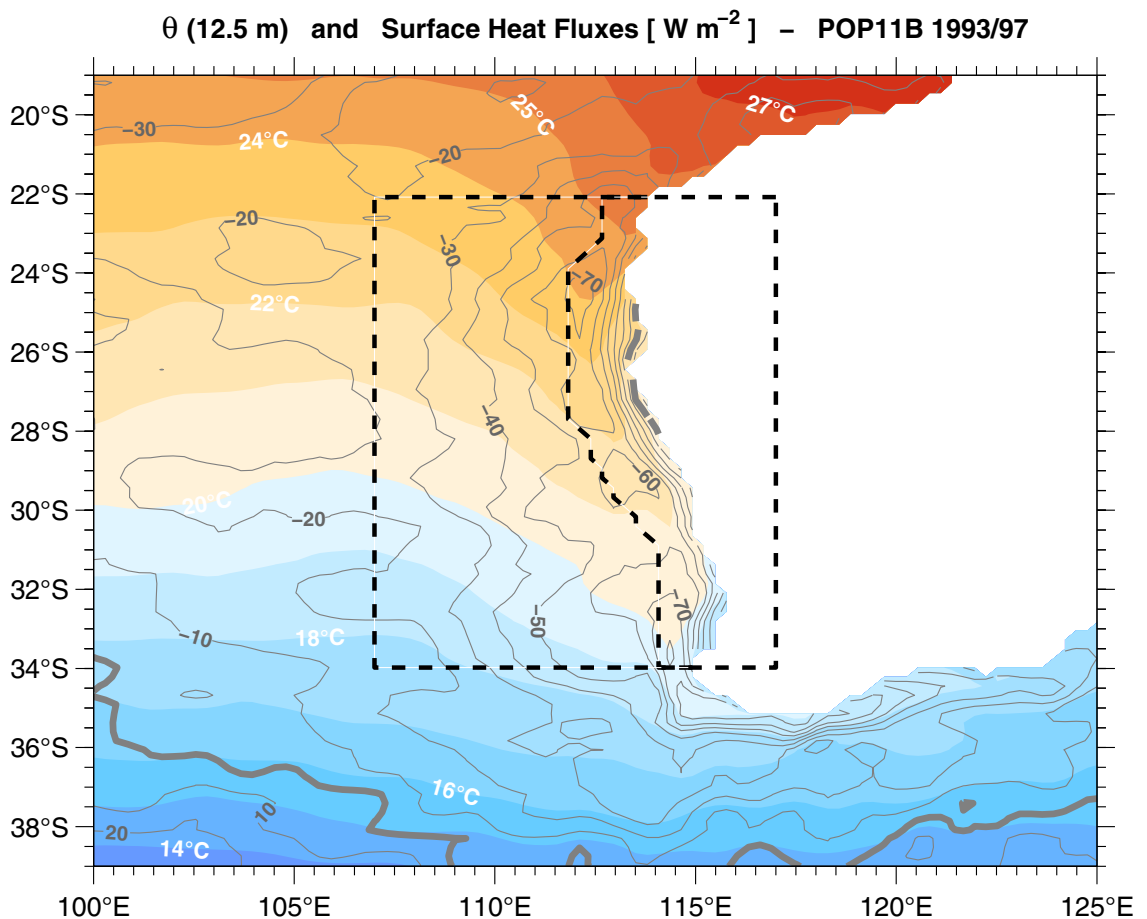


Figure 6.1. Net surface heat fluxes and potential temperature (θ) in the southeast Indian Ocean over a 5-year mean period between 1993/97. Ocean heat loss is negative. The dotted lines define the coastal and the offshore boxes used in the heat budget calculations.

6.3.1 Coastal and offshore boxes

The estimates of the heat balance for the coastal box are given in **Table 6.1**. The balance is primarily achieved between the surface flux, the mean and the eddy divergence terms. The large mean heat convergence (221 W m^{-2}) is balanced by the surface cooling (-48 W m^{-2}) and also laterally by the eddy divergence (-175 W m^{-2}). The eddy divergence explains $\sim 80\%$ of the cooling of the mean flow. The mean convergence and eddy divergence are greatest in the upper 310 m, at depths of the Leeuwin Current and Leeuwin Undercurrent [**Figure 6.2**, top panel]. The maximum heat convergence occurs near surface (top 37.5 m) followed by a secondary maximum at 160 m. As the eddy divergence mainly balances the mean convergence, its vertical profile tends to be a mirror image of the mean, except in the model “mixed layer” where the surface flux removes part of the mean ocean heat to the atmosphere.

Table 6.1. **Heat balance in the coastal and offshore boxes defined in Figure 6.1.**

HEAT BUDGET			Box	
			OFFSHORE	COASTAL
	Net surface heat flux	[W m^{-2}]	-37	-48
$\nabla\langle\mathbf{U}\Theta\rangle$	Total ocean heat convergence	[W m^{-2}]	38	44
$\nabla\langle\mathbf{U}\rangle\langle\Theta\rangle$	Mean ocean heat divergence	[W m^{-2}]	10	221
$\nabla\langle\mathbf{U}'\Theta'\rangle$	Eddy ocean heat div/convergence	[W m^{-2}]	28	-175
$\nabla\langle\mathbf{U}_s'\Theta_s'\rangle$	Seasonal ocean heat divergence	[W m^{-2}]	0	-2
$\nabla\langle\mathbf{U}_i'\Theta_i'\rangle$	Interannual ocean heat divergence	[W m^{-2}]	0	0
$\nabla\langle\mathbf{U}_s'\Theta_i'\rangle$	Mixed ocean heat divergence	[W m^{-2}]	0	0
$\nabla\langle\mathbf{U}_i'\Theta_s'\rangle$	Mixed ocean heat divergence	[W m^{-2}]	0	0
	Storage + diffusion	[W m^{-2}]	1	-4
	Net volume (mass) flux	[kg m^{-3}]	0.01	0.03
	Box surface area	[10^{12} m^2]	0.80	0.24

* Heat and volume fluxes into the ocean box are positive

In the ocean interior adjacent to the Leeuwin Current (offshore box), the heat balance is again primarily between the surface flux, the mean and the eddy divergence terms [**Table 6.1**]. Now, however, both the mean flow (10 W m^{-2}) and the eddy (28 W m^{-2})

heat the box whereas the surface flux cools it (-37 W m^{-2}). So the eddy flux warms the ocean in this offshore box instead of cooling as in the coastal box, and it basically converges 2.8 times more heat than the mean ($\sim 70\%$ of the warming). The mean convergence occurs mainly in the upper 62.5 m but most strongly at surface (12.5 m) [Figure 6.2, bottom panel]. Below 62.5 m and above 150 m, the mean flow actually exports heat from the box. The eddy convergence has a maximum at 62.5 m but it is still reasonably significant in the upper 160 m. The shallower influence of the mean and eddy fluxes, compared to the upper 310 m in the coastal box, is likely explained by the deepening of isopycnals near the coastal boundary. We note that in both the coastal and offshore boxes the seasonal cycle and interannual processes play a relatively minor role in the heat balance.

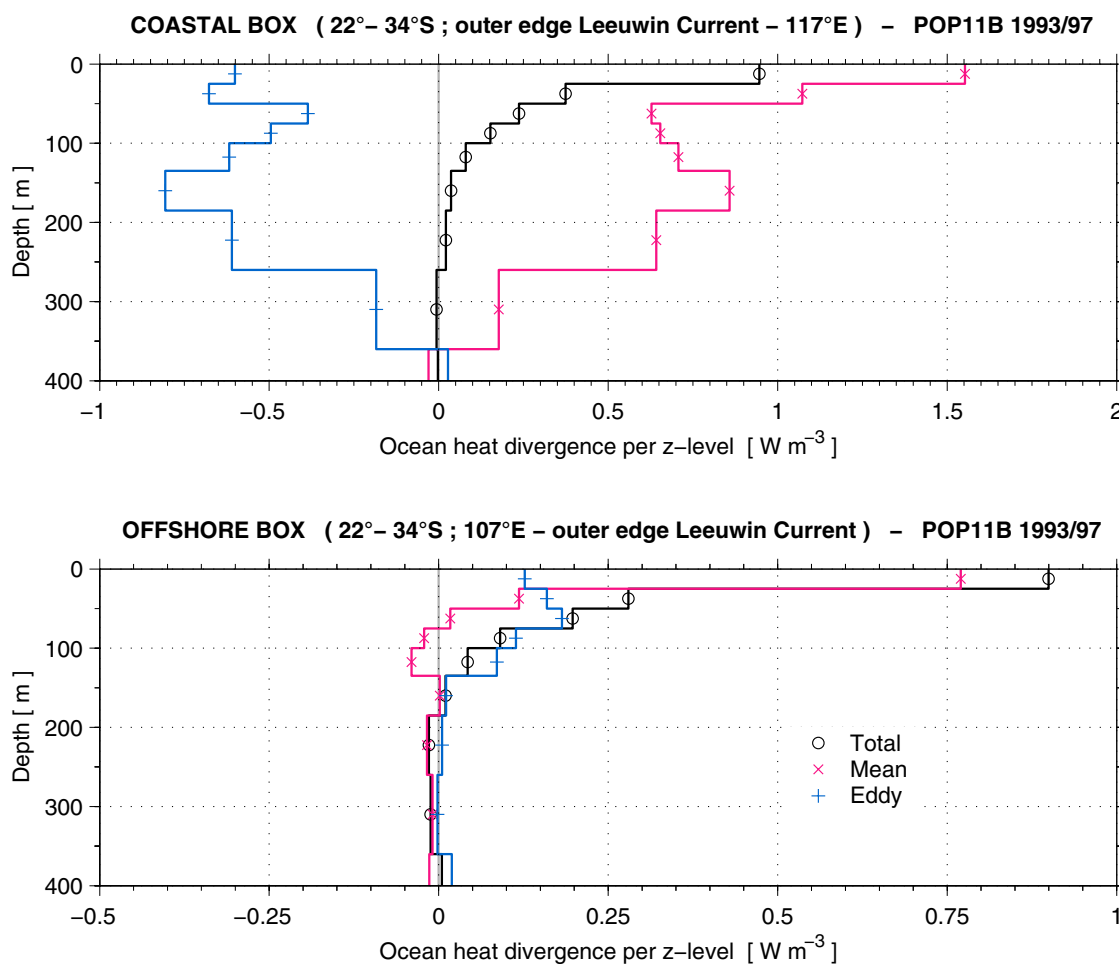


Figure 6.2. Total, mean and eddy heat divergence per model z-level in the upper 400 m, for the coastal box (top panel) and offshore box (bottom panel), both depicted in Figure 6.1. The model z-level thicknesses are detailed in Appendix C.

6.3.2 Regional overview

A large scale composite of the dominant terms of the heat balance off Western Australia was constructed using a series of $1^\circ \times 1^\circ$ boxes for the ocean region between $20^\circ\text{--}38^\circ\text{S}$ and $100^\circ\text{--}125^\circ\text{E}$. The composite comprises the surface flux [Figure 6.3] and the total ocean divergence [Figure 6.4]. Though a top-to-bottom integration was performed, we only show the ocean heat divergence in the upper 185 m, which is representative of Leeuwin Current depths and which also captures the bulk of the heat divergence. In general, between 22°S and 34°S , the ocean flows bring heat into the area which is then removed through the surface to the atmosphere. This occurs more intensely along the mean path of the Leeuwin Current, and also in locations adjacent to its outer edge where mesoscale eddies are highly active. The similarity of Figures 6.3 and 6.4 means that even on this small scale, storage+diffusion is rather weak [see Appendix D for storage+diffusion and mass flux details].

The total ocean heat divergence [Figure 6.4] primarily results from the balance between the mean [Figure 6.5] and eddy [Figure 6.6] terms. The mean flow accumulates heat mainly along the path of the Leeuwin Current where some “convergent hot spots” are evident. Eddies then remove the heat from the Leeuwin Current and transfer it to the offshore ocean. The comparison between the strong eddy divergence near the coast with its broader and weaker associated convergence in the ocean interior suggests that eddies carrying heat are formed in a narrow strip along the Leeuwin Current’s edge, but the eddies and their heat cargo are dissipated over a much broader area. In fact, the eddy fluxes are removing heat from the mean Leeuwin Current along its poleward path [Figure 6.7] and spreading it to the ocean interior in a broadly coherent southwestward direction, in other words, down the mean θ gradient [Figure 6.8]. This lateral spreading of the heat offshore effectively allows the air–sea fluxes to cool the ocean over a larger area.

More details of the heat balance can be understood from the schematic diagrams drawn in Figure 6.9, for the mean and eddy fluxes associated with the coastal and offshore boxes, above and below 185 m. Although the Leeuwin Current extends down to 300 m near 34°S , at this same depth near 22°S , one finds the equatorward Leeuwin Undercurrent. So, to avoid misinterpretation we have chosen the upper 185 m as representative of the Leeuwin Current. Firstly, we observe that the convergence of the mean heat (39 TW) in the coastal box is only 12% of the total amount being advected into the box (324 TW), so most part of the heat input is fluxed out through the southern (–163 TW) and bottom (–122 TW) sections of the box. Note that, the mean flow through the bottom of the box is most explained by the model z -level cutting across isopycnals sloping more strongly near the coast. Secondly, the mean heat convergence (39 TW) is balanced by heat loss to the atmosphere (~30%, –12 TW) and by lateral transfer to the

offshore ocean through divergence of the eddy fluxes (~70%, -28 TW). So the above implies that from the 6°C cooling of the mean Leeuwin Current, observed between 22°S and 34°S [**Chapter 5**], the eddy flux divergence accounts for at least for 4°C. Thirdly, overall, the eddy heat fluxes from the coastal box laterally transfer 43 TW to the offshore box, however, only ~50% (20 TW) of this heat stays in the offshore box to be cooled by the surface flux. The other half is spread elsewhere (-5 TW equatorward, -8 TW westward and -7 TW poleward) [**Figure 6.9**].

6.3.3 Westward eddy heat flux

The eddy field in the ocean adjacent to the west Australian coast is a conspicuous part of the regional circulation [Morrow and Birol, 1998]. The most impressive feature of this field is the long lived warm core anticyclonic eddies which detach from the boundary flow of the Leeuwin Current and migrate westward into the ocean interior. The annual average estimate of the westward eddy heat flux associated with these warm core eddies is 4 to 5 TW, in the upper 1500–2500 m [Morrow *et al.*, 2003]. By integrating the westward eddy heat flux down to 1500–2500 m in the model [**Appendix D**] we obtain 43 TW [equivalent to the full 0–5200 m depth integration, see coastal box in **Figure 6.9**], an estimate which is about 10 times greater than what has been measured by Morrow *et al.* [2003]. Even if we integrate down to depths (upper 185 m) representative of the Leeuwin Current, we still obtain a much larger value of 26 TW [coastal box in **Figure 6.9**].

In addition to the above magnitude differences, we observe another two disagreements between the westward eddy heat fluxes in the model and those associated with the long lived warm core eddies. First we note that the warm core eddies preferentially propagate northwestward along isopycnals corridors [Fang and Morrow, 2003] whereas the model eddy heat fluxes move southwestward across isothermals [**Figure 6.8**]. A second discrepancy is that the long lived warm core eddies detach from the Leeuwin Current at seasonal timescales, mainly during May–July and, although, this is seen in the model [see sea level anomalies in **Chapter 5**], the Reynolds decomposition of the heat balance clarifies that the model eddy heat fluxes are driven by processes operating at submonthly timescales and that seasonal rectification is not significant [**Table 6.1**].

Using the LUCIE mooring array measurements at ~29°S, Feng *et al.* [2005b] determined a pointwise estimate for the westward eddy heat flux of about $3.2 \cdot 10^7 \text{ W m}^{-1}$ over the 0–200 depth range. If we integrate this value over ~1350 km distance, from North West Cape (22°S) to Cape Leeuwin (34°S), we obtain 44 TW. Then if we consider Feng's *et al.* 50% factor, the estimate decreases to 22 TW. Their 50% factor was introduced to account for spatial variations of the eddy field. Thereby the magnitude of

the westward eddy heat flux over the entire distance of the west Australian coast must vary from 22 to 44 TW, a range in the same order of the model estimate (26 TW).

The agreement in the order of magnitude of the model westward eddy heat flux with Feng's *et al.* estimate and the disagreement with the value associated with the long lived warm core eddies suggest that the long lived warm cores eddies are not the dominant eddy mechanism removing heat from the mean Leeuwin Current and that they may only account for 10% of the total amount. In fact, Morrow *et al.* [2003] recognise that they have only considered the long lived anticyclonic eddies and have not addressed the role of short lived warm or cold core eddies, which also populate the ocean interior off Western Australia. Although the model heat balance does not give any clues about the submonthly timescale processes generating the westward eddy heat fluxes, we believe that the short lived warm core eddies are a strong contender. These short lived warm eddies are generated in different times of the year, are mostly spawned south of 31°–33°S, and dissipate quickly (east of 110°E) as they move westward/southwestward [Fang and Morrow, 2003]. Their pathways in Morrow *et al.* [2004] (their Figure 1) seem quite consistent with the broad southwestward spreading of the model eddy heat flux in **Figure 6.8**.

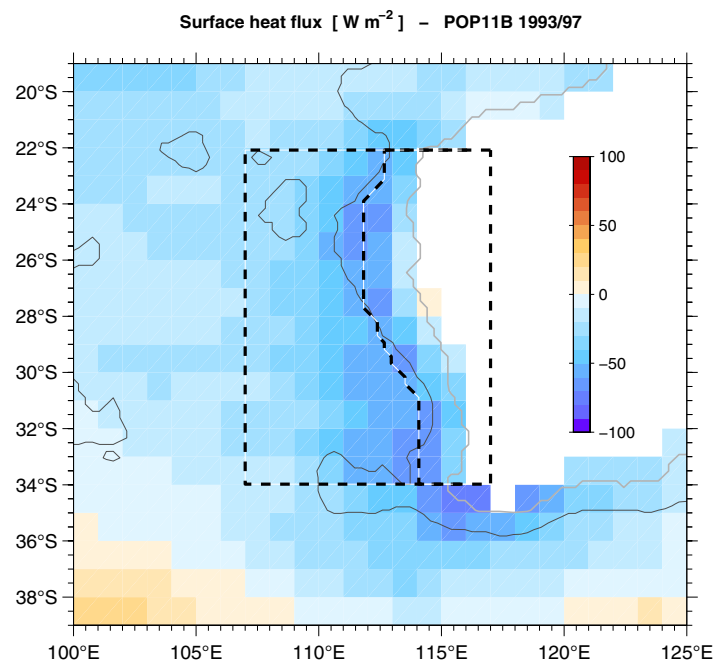


Figure 6.3. Net surface heat fluxes over $1^\circ \times 1^\circ$ grid boxes. Ocean heat loss is negative (blue). The thin black line is the 3000 m isobath. The gray line defines the model coastline.

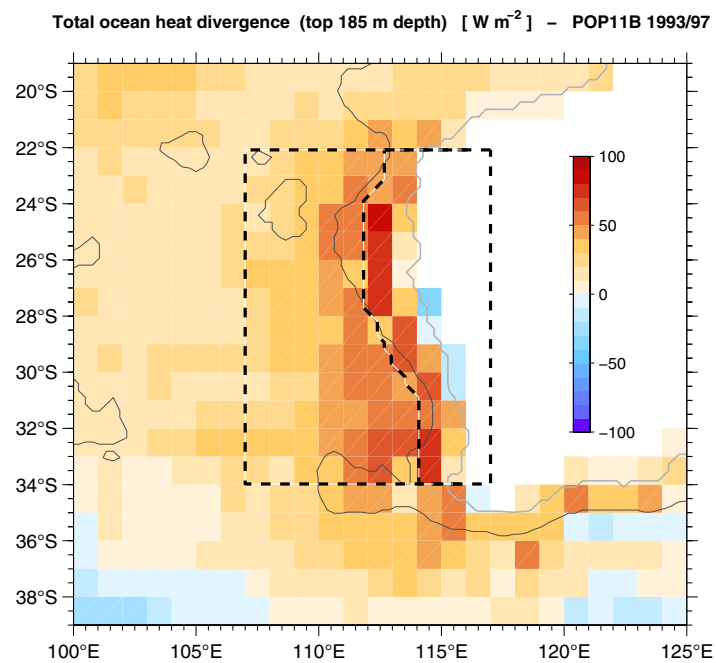


Figure 6.4. Total ocean heat divergence over $1^\circ \times 1^\circ$ grid boxes. Ocean heat gain is positive (red). The thin black line is the 3000 m isobath. The gray line defines the model coastline.

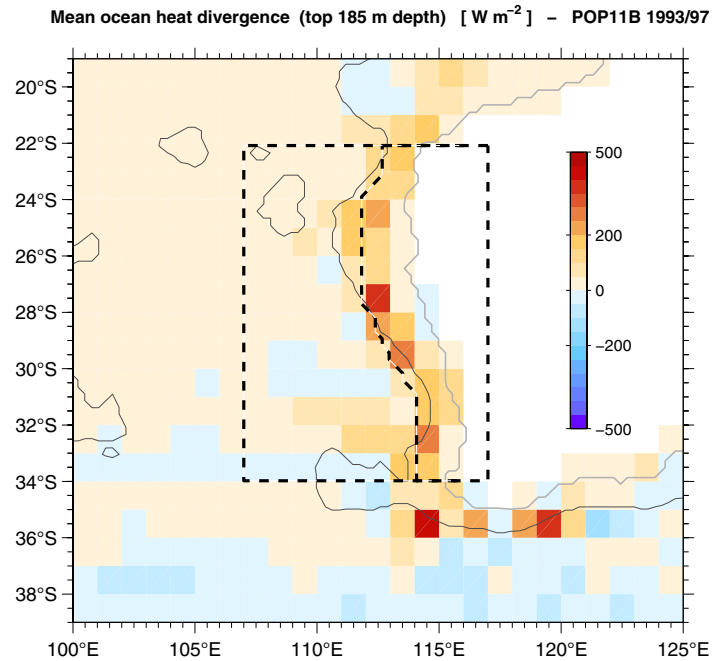


Figure 6.5. Mean ocean heat divergence over $1^\circ \times 1^\circ$ grid boxes. Ocean heat gain is positive (red). The thin black line is the 3000 m isobath. The gray line defines the model coastline.

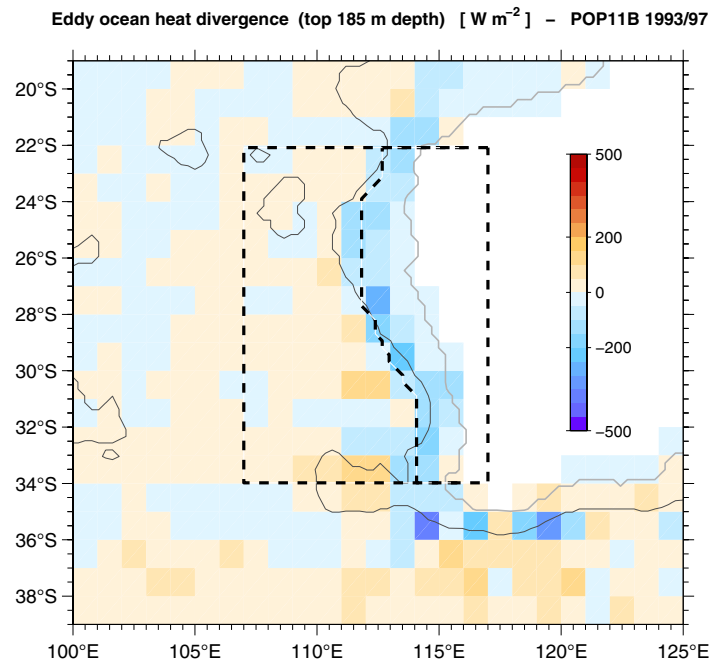


Figure 6.6. Eddy ocean heat divergence over $1^\circ \times 1^\circ$ grid boxes. Ocean heat gain is positive (red). The thin black line is the 3000 m isobath. The gray line defines the model coastline.

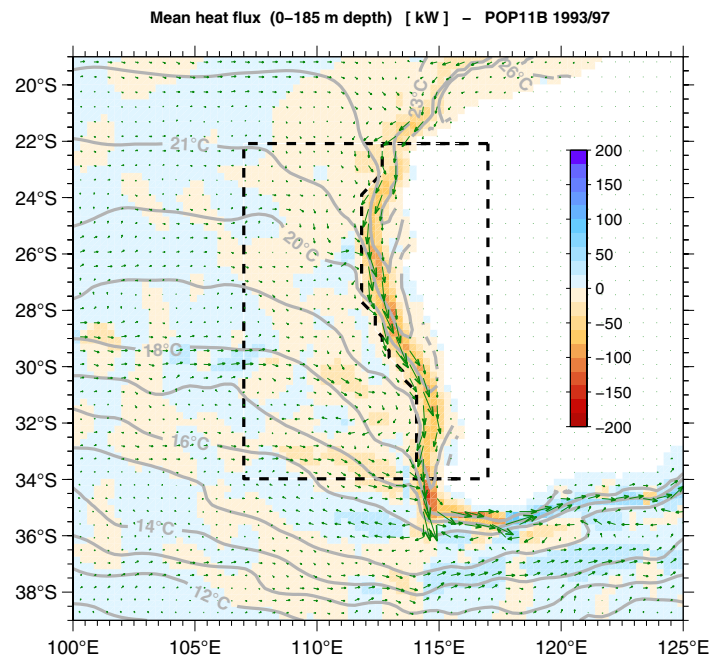


Figure 6.7. Mean ocean heat fluxes (every second vector plotted) and potential temperature (θ) in the upper 185 m of the southeast Indian Ocean averaged over a 5-year period between 1993/97. The colour indicates the absolute mean heat flux with the sign of the meridional component (N+).

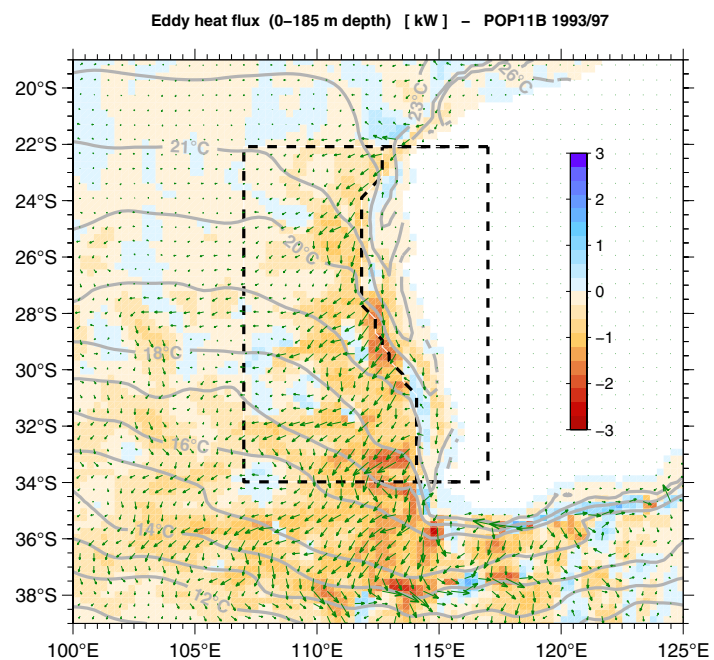


Figure 6.8. The same as in **Figure 6.7** but for the eddy ocean heat fluxes.

Heat budget - POP11B 1993/97

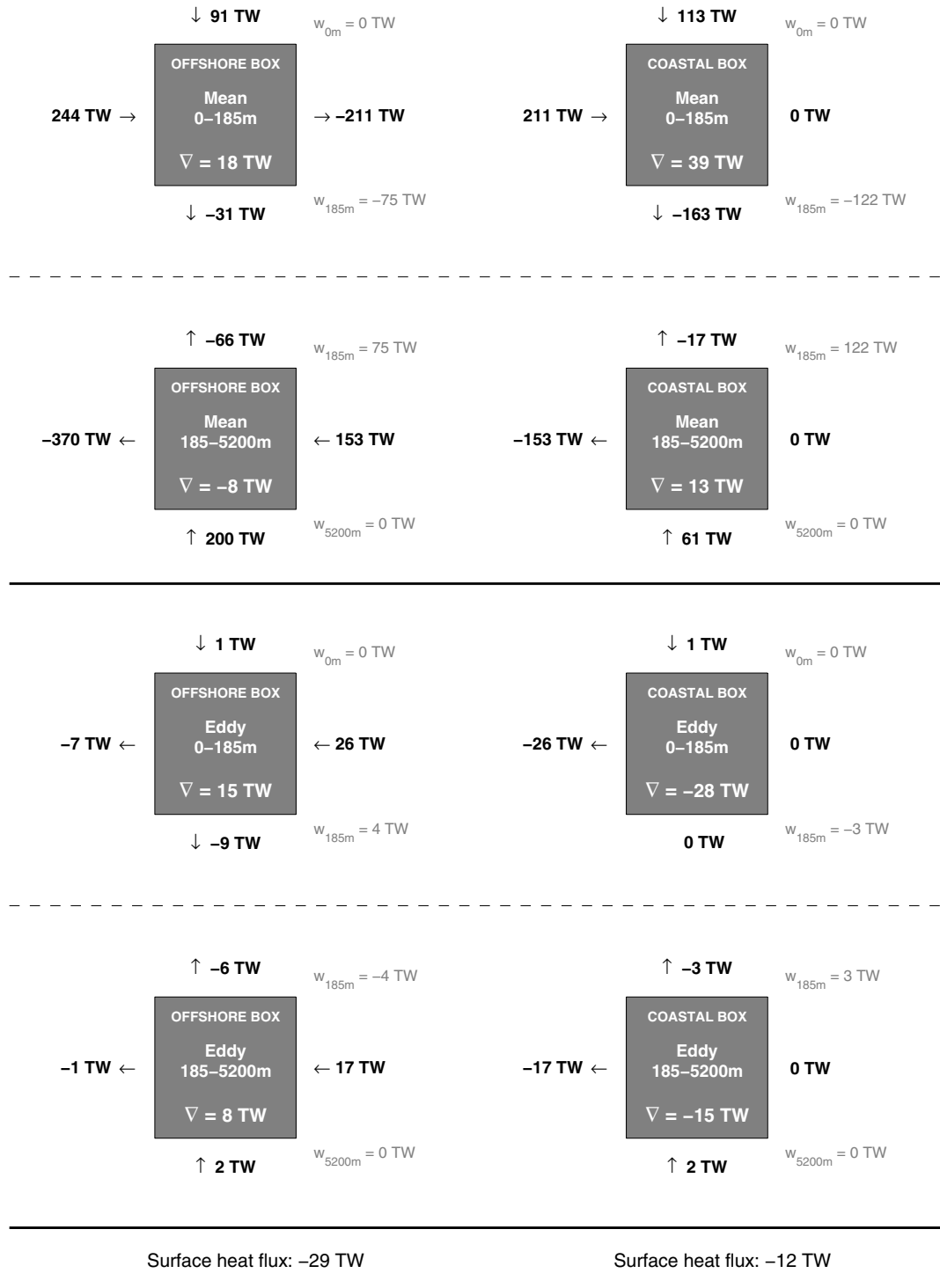


Figure 6.9. Schematic diagrams for the mean and eddy heat fluxes in the coastal and offshore boxes [Figure 6.1], above and below 185 m depth.

6.4 CONCLUSIONS

In the fairly realistic POP11B simulation it is the divergence of eddy heat flux associated with submonthly processes which is the dominant mechanism cooling the mean Leeuwin Current between 22°S and 34°S: about 4°C out of 6°C (~70% drop in jet temperature). Heat is converged by the mean flow and then transferred to the adjacent ocean interior by eddy flows. This implies a minor role for the air–sea fluxes in the local cooling of the Leeuwin Current, and thus possibly for vertical mixing (convection) which was suggested to create deep mixed layers and consequently to maintain the mean poleward flow of the Leeuwin Current against the opposing equatorward wind stress [e.g., Thompson, 1984].

While the eddy heat fluxes originate in a narrow region at the outer edge of the Leeuwin Current, they radiate across isotherms to the southwest and “dump” their heat over a much larger area of the southeastern Indian Ocean compared to where they are generated. This effectively “smears” the lateral temperature gradients in the region, thus the broad wedge of warm water associated with the mean climatological Leeuwin Current is maintained, not by a broad mean flow, but by a narrow flow diffusing heat laterally due to eddy fluxes. Hence, eddies are not just key to the Leeuwin Current momentum balance as shown in Feng *et al.* [2005b], they are also critical for its heat balance.

About half of the heat removed from the boundary and transferred to the ocean interior by the eddy flux divergence remains in the region (offshore box) to be cooled by the air–sea fluxes, which now have a vast area over which to operate. The other half is transferred out of the region by eddy flows and spread equatorward, westward and poleward. The divergence of the eddy heat flux is responsible for ~70% of the warming of the ocean interior offshore of the Leeuwin Current. The other ~30% is accounted for the mean convergence.

In the model, the westward eddy heat flux carry about 43 TW (or 26 TW at Leeuwin Current depths). The model 26 TW is in the same order of magnitude of Feng’s *et al.* [2005b] estimate extrapolated to the entire west Australian coast (22–44 TW). In observations, only 4 to 5 TW seem associated with long lived warm core eddies which detach from the Leeuwin Current [Morrow *et al.*, 2003]. This suggests that other eddy motion must play an important role in the lateral transfer of heat. We believe the more likely contender is the short lived warm core eddies.